

Study of some micro-structural phenomena in granular shear zones

Jan Kozicki, Jacek Tejchman, and Danuta Leśniewska

Citation: *AIP Conf. Proc.* **1542**, 495 (2013); doi: 10.1063/1.4811976

View online: <http://dx.doi.org/10.1063/1.4811976>

View Table of Contents: <http://proceedings.aip.org/dbt/dbt.jsp?KEY=APCPCS&Volume=1542&Issue=1>

Published by the [AIP Publishing LLC](#).

Additional information on AIP Conf. Proc.

Journal Homepage: <http://proceedings.aip.org/>

Journal Information: http://proceedings.aip.org/about/about_the_proceedings

Top downloads: http://proceedings.aip.org/dbt/most_downloaded.jsp?KEY=APCPCS

Information for Authors: http://proceedings.aip.org/authors/information_for_authors

ADVERTISEMENT



AIP Advances

Submit Now

Explore AIP's new
open-access journal

- Article-level metrics now available
- Join the conversation! Rate & comment on articles

Study of Some Micro-Structural Phenomena in Granular Shear Zones

Jan Kozicki¹, Jacek Tejchman¹ and Danuta Leśniewska²

¹*Gdansk University of Technology, Gdansk-Wrzeszcz, Poland*

²*Koszalin University of Technology, Koszalin, Poland*

Abstract. The paper deals with some characteristic phenomena of fundamental nature which occur within shear zones in granular materials. Phenomena such as self-organizing force chain networks, vortices, alternating contractant and dilatant regions within shear zones were modelled numerically using discrete element method DEM. Discrete simulations were carried out with medium-dense sand during direct a shearing test.

Keywords: Shear localization, DEM, Granular Material, Direct Shear Test, Triaxial Test, Contact Moments

PACS: 45.70._n

INTRODUCTION

Shear localization is a fundamental phenomenon in geomaterials. Recent experimental works indicate [1]-[3] some characteristic and remarkable phenomena of fundamental nature which occur within shear zones, such as: self-organizing force chain networks, vortices, micro-bands, buckled granular columns, alternating contractant and dilatant regions.

The objective of the paper is to examine numerically some micro-structural events (e.g. force chains, vortex structures, local void ratio fluctuations, strain non-uniformities) in real cohesionless sand (so-called Karlsruhe sand) by means of the discrete element method DEM. The events were investigated base on a direct shear test which is a very popular laboratory test widely used in soil mechanics, rock mechanics and mechanics of bulk solids to determine some important properties of cohesionless and cohesive materials such as: drained strength envelope, flow function, angle of internal friction, dilatancy angle, wall friction angle and cohesion. To simulate the sand behaviour, the three-dimensional spherical discrete model YADE developed at University of Grenoble was used, allowing for introducing grain rolling resistance in order to take into account the grain roughness and using a linear contact model [4]. The particle breakage was not considered since the assumed pressure level was small. The discrete element modelling results were also directly compared with the finite element results based on a micro-polar hypoplastic constitutive model [5] for the same sand,

initial void ratio, pressure, specimen size and test boundary conditions.

CALIBRATION OF DISCRETE PARAMETERS

In the paper, spherical elements were used only. To simulate sand grain roughness, additional moments were introduced into the 3D spherical model [4], which were transferred through contacts and resisted particle rotations. Our discrete element model can simulate the different grain shape by using different symmetric and non-symmetric clusters of spheres [6], we chose however spheres with contact moments for 2 reasons: a) in order to significantly shorten the computation time (calculations with spheres possessing contact moments are 3-5 times faster than those using complex clumps [7]) and b) in order to directly compare the discrete results with the finite element results based on a micro-polar approach. Pasternak and Mühlhaus [8] demonstrated that the additional rotational degree of freedom of a micro-polar continuum arose naturally by mathematical homogenization of an originally discrete system of spherical grains with contact forces and moments. Therefore, the choice of spheres in discrete simulations was intentional.

The following five main local material parameters were needed for discrete simulations using a linear contact model: E_c , ν_c , μ , β and η . (E_c - modulus of elasticity of the grain contact, ν_c - Poisson's ratio of the grain contact, μ - the inter-particle friction angle, β

- rolling stiffness coefficient and η - rolling coefficient controlling the limit of the rolling behaviour). In addition, the particle radius R , particle density ρ and damping parameters α were required. The material parameters were calibrated with the corresponding axisymmetric triaxial laboratory test results for Karlsruhe sand [9]. The index properties of Karlsruhe sand are: mean grain diameter $d_{50}=0.50$ mm, grain size among 0.08 mm and 1.8 mm, uniformity coefficient $U=2$, maximum specific weight $\gamma_d^{max}=17.4$ kN/m³, minimum void ratio $e_{min}=0.53$, minimum specific weight $\gamma_d^{min}=14.6$ kN/m³ and maximum void ratio $e_{max}=0.84$. The sand grains are classified as sub-rounded/sub-angular. The height and diameter of the sand specimen were 100 mm.

In numerical simulations [6], a cubical sand specimen of $10 \times 10 \times 10$ cm³ was used. A simplified linear grain distribution curve was assumed, namely, the grain range was among 2.5 mm and 7.5 mm with $d_{50}=5.0$ mm instead of $d_{50}=0.5$ mm for real Karlsruhe sand). The tests were modelled using confining smooth rigid wall elements (without inducing non-homogeneous deformation). The top and bottom boundaries moved vertically as loading platens under strain-controlled conditions to simulate the confining pressure p . The following material parameters were assumed in discrete simulations: $E_c=0.3$ GPa, $\nu_c=0.3$, $\mu=18^\circ$, $\beta=0.7$ and $\eta=0.4$ and $\rho=2.6$ kN/m³, $\alpha=0.08$ and $d_{50}=5.0$ mm to match the experimental results for real sand [9].

Figure 1 shows the calculated evolution of the vertical normal stress σ_l and volumetric strain ϵ_v versus vertical normal strain ϵ_l for spheres with contact moments during triaxial compression with initially dense sand ($e_o=0.53$, $d_{50}=5$ mm) as compared to the laboratory experiments [9] at one arbitrary confining pressure $\sigma_c=200$ kPa.

From DEM it can be seen that the initially dense specimen exhibits initially elasticity, hardening (connected first to contractancy and then dilatancy), reaches a peak at about of $\epsilon_l=6\%$, (that is in accordance with the experiment) gradually softens and dilates reaching at large vertical strain of 25% a critical state. The global macroscopic elastic parameters are: $E=70$ MPa and $\nu=0.25$. The calculated E -value is slightly smaller than the experimental one of 100 MPa. The global maximum mobilized internal friction angle (calculated with principal stresses from the Mohr's equation) is $\phi_{max}=42^\circ$ and is the same as the experimental value of $\phi_{max}=42^\circ$. The calculated dilatancy angle of $\psi=30^\circ$ with spheres with contact moments matches very well the experimental outcome of $\psi=28.5^\circ$. In turn, the calculated global residual internal friction angle is $\phi_{cr}=35^\circ$, respectively. The granular system shows small fluctuations in the residual phase. Summarized, the discrete results with

spheres and contact moments are in a satisfactory accordance with experiments.

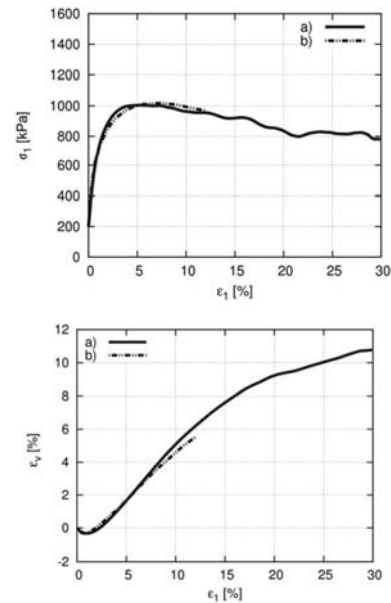


FIGURE 1. Vertical normal stress σ_l versus vertical normal strain ϵ_l and volumetric strain ϵ_v versus ϵ_l during triaxial compression test ($e_o=0.53$, $\sigma_c=200$ kPa): a) discrete results with spheres, contact moments and linear contact model ($E_c=0.3$ GPa, $\nu_c=0.3$, $\mu=18^\circ$, $\beta=0.7$, $\eta=0.4$, $d_{50}=5.0$ mm), b) experimental results with $d_{50}=0.5$ mm [9].

DISCRETE RESULTS OF DIRECT SHEAR TEST

In a real direct shear test performed in Karlsruhe University with Karlsruhe sand, the sand specimen was $100 \times 100 \times 20$ mm³ [9]. In discrete 2D calculations, a sand specimen with a length of $l=100$ mm and a height of $h=20$ mm ($l/h=5$) was assumed as in the experiment. The specimen depth varied between the grain size and 20 mm. The vertical displacement along the top edge of the upper box was free but constrained to move by the same amount. The same horizontal velocities were prescribed to the entire upper box half (the lower part was fixed).

In discrete simulations, the spheres had a diameter, linearly varying between 0.25 and 0.75 mm (the mean grain diameter was the same as in the real sand, $d_{50}=0.5$ mm). Initially, the top moved downwards vertically as loading platens under strain-controlled conditions to simulate the lateral pressure $p=100$ kPa. The initial spatial void ratio of a medium dense sand specimen was $e_o=0.60$ (similar as in FE calculations

[5]). The calculations were carried out with the parameters determined during a triaxial test: $E_c=0.3$ GPa, $\nu_c=0.3$, $\mu=18^\circ$, $\beta=0.7$ and $\eta=0.4$ and $\rho=25.5$ kN/m³, $\alpha=0.08$ and $d_{50}=0.5$ mm. In total, 22'000 spheres were used with the specimen depth equal to the grain size.

Figure 2 presents the calculated evolution of the resultant (global) horizontal shear force T and vertical normal force N and evolution of the vertical displacement of the top edge u_v versus the normalized horizontal displacement of the upper box u/h (h – height of the specimen). The calculated global horizontal force T has a typical evolution character for initially dense and medium dense granulates during direct shearing [10]; it grew from the beginning of shearing, reached the maximum at $u=0.5$ mm ($u/h=0.025$), showed pronounced softening and tended to an asymptotic value at $u=5$ mm ($u/h=0.20$). The calculated overall internal friction angle, $\varphi=\arctan(T/N)$, was equal to $\varphi^p=42^\circ$ at peak and approximately $\varphi_{res}=32^\circ$ at residual state. In laboratory experiments with the same sand, specimen height and length and initial void ratio under the same vertical pressure of $p=100$ kPa, the values of φ were slightly higher: $\varphi^p=45.5^\circ$ (at peak) and $\varphi_{res}=37^\circ$ (at residual state) [10]. The experimental outcomes are slightly higher since the calibration procedure was solely performed with $d_{50}=5$ mm (not with $d_{50}=0.5$ mm).

After initial contractancy due to the applied load p , the top edge slightly lowered and then lifted due to dilatancy accompanying shearing - later the boundary displacement reached an asymptote.

The calculated normalized vertical displacement of the top boundary was $u_v/h=0.045$ ($u_v=0.90$ mm) at $u/h=0.5$ ($u=10$ mm). This value is larger than in the experiment ($u_v/h=0.035$ at $u/h=0.5$ ($u=10$ mm) [10]. The horizontal force and volume change reached a constant value at the residual state besides some fluctuations caused by a continuous reorganization of grain force chains during shearing.

A pronounced horizontal shear zone appeared in the specimen mid-region, which was characterized by the occurrence of shear strain (Fig.3a) and grain rotations ω (Fig.3b). The direction of the resultant rotation ω^c (from the area $5d_{50}\times 5d_{50}$) was in accordance with the shearing direction. The shear zone started to appear at about $u=1.0$ mm, after the force peak. In the specimen centre, the thickness of a shear zone was about $t_s=11$ mm ($22\times d_{50}$) on the basis of shear deformation (Fig.3a).

The evolution of the contact network in the shear box is demonstrated in Fig.4a. The colour intensity represents the different compressive normal contact force between two particles. The distribution of internal contact forces is non-uniform and

continuously changes. Force chains of heavily loaded grain contacts bear and transmit the compressive load on the entire granular system and are the predominant structure of internal forces at micro-scale. The internal stresses are supported mainly along the direction of the diagonal going from the upper left to the lower right of the box (opposite to the shear direction). Thus, the anisotropy of the test is very strong. The distribution of void ratio across the shear zone is strongly non-uniform, alternating in a nearly periodic fashion (Fig.4b). The specimen globally dilates in the shear zone, however the local void ratio may also contract.

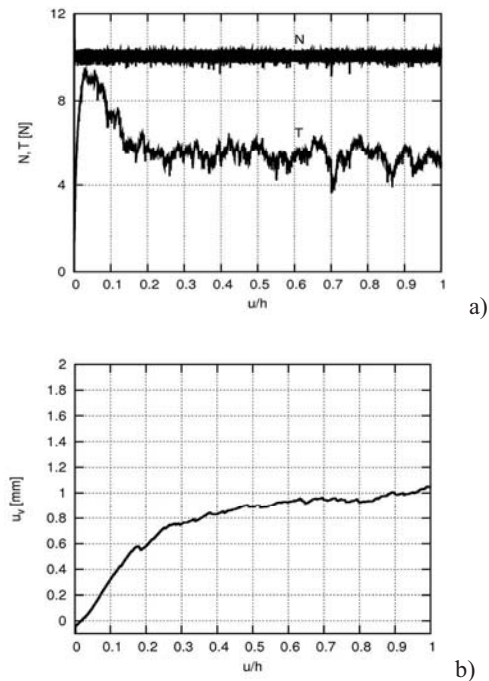


FIGURE 2. DEM results of direct shearing of initially medium dense sand ($e_o=0.60$, $d_{50}=0.5$ mm): a) evolution of resultant horizontal shear force T and vertical normal force N on top edge versus normalized horizontal displacement of top edge u/h , b) evolution of vertical displacement of top edge u_v versus u/h .

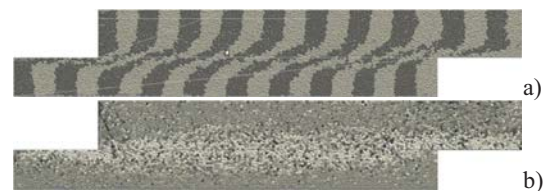


FIGURE 3. Distribution of deformation (a) and grain rotations (b) in initially medium dense sand ($e_o=0.60$, $d_{50}=0.5$ mm) from DEM at $u/h=1.0$ ($u=20$ mm).

Figure 4c presents a spontaneous occurrence of displacement fluctuations in the shear zone in the form of clusters of circulating cells (so-called vortex structures) observed in real experiments [1], [2]. The map of Fig.4c was obtained by drawing the displacement difference vector for each sphere with respect to the background translation corresponding to the homogeneous (affine) strain. The individual particle displacements are able to form large long-range deformation vortex structures, wherein cells rotate as a rigid body whereas the space between them is characterized by intense relative rotations. This leads to clusters of rotational bearings and zones of intense slippage. The vortex-like patterns are well recognized in particular at the residual state. The three vortices occurred with the diameter of about the shear zone thickness (10 mm) at the distance equal to the specimen height (20 mm). These fluctuation loops are connected closely with force chains, alternating changes of local void ratio and global macroscopic stress fluctuations [1]. They are a direct manifestation of grain rearrangement [2].

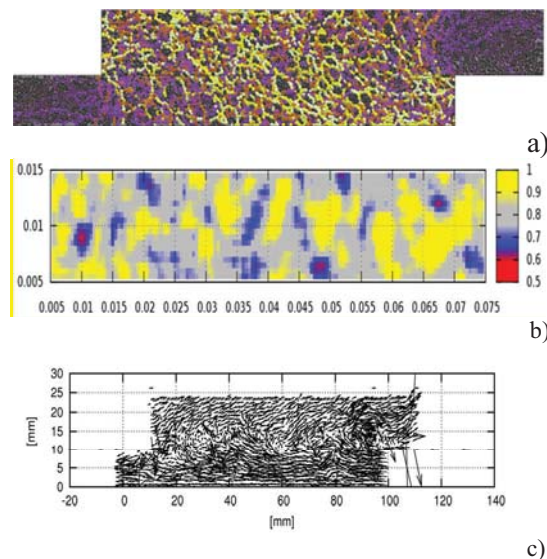


FIGURE 4. DEM results of direct shearing of initially medium dense sand ($e_0=0.60$, $d_{50}=0.5$ mm): a) distribution of internal forces in specimen, b) distribution of void ratio in shear zone, c) distribution of vortex structures in specimen during normalized horizontal displacement of top edge $u/h=1$.

The DEM modelling results were similar to those obtained with the FEM based on a micro-polar hypoplastic constitutive model [5] with respect to global macro-quantities. Some discrepancies existed with respect to micro-parameters: the magnitude and evolution of the micro-polar rotation and the magnitude of material dilatancy.

CONCLUSIONS

During direct shear test, the deformations and stresses are strongly non-affine. The thickness and shape of the shear zone appearing along a horizontal mid-section are also non-uniform. The shape of the shear zone is close to a horizontal plane. The shear zone is the widest in the mid-region. In the shear zone, vortex structures and local void ratio fluctuations systematically occur that seem to have a periodically organised structure. Their precise link with non-stable force chains and force cycles merit further investigations in order to develop advanced physics-based models for granular materials undergoing shear.

The largest internal work during shearing is performed by contact tangential forces and the smallest one by normal forces. The transitional kinetic energy is 10 times higher than the rotational one. The overall internal friction angle and volume changes increase with increasing μ and β and decreasing η .

At the elastic stage, the boundary external work is mainly converted into the elastic energy. At the residual state, it is mainly dissipated by plastic deformation. The evolution of the elastic energy is inherently related to the dilation effect that reduces the normal contact forces and contact point number.

ACKNOWLEDGMENTS

The research work was funded by the Polish National Science Centre (nr DEC-2011/03/B/ST8/05865).

REFERENCES

1. S. Abedi, A. L. Rechenmacher and A. D. Orlando, *Granular Matter* **14**, 6, 695-705, (2012).
2. V. Richefeu, G. Combe and G. Viggiani, *Geotechnique Letters* **2**, 113-118 (2012).
3. D. Leśniewska, M. Niedostatkiewicz and J. Tejchman, *Strain* **47**, 2, 218-231 (2012).
4. J. Kozicki and F. V. Donze, *Computer Methods in Applied Mechanics and Engineering* **197**, 4429-4443 (2008).
5. J. Tejchman and E. Bauer, *Computers and Geotechnics* **21**, 1, 1-16 (2005).
6. J. Kozicki, J. Tejchman and Z. Mróz, *Granular Matter* **14**, 4, 457-468 (2012a).
7. J. Kozicki, J. Tejchman and Z. Mróz, *Acta Geotechnica* 2012b (under review).
8. E. Pasternak and H.-B. Mühlhaus, *Journal of Engineering Mathematics* **52**, 1, 199-229 (2005).
9. W. Wu, "Hypoplastizität als mathematisches Modell zum mechanischen Verhalten granularer Stoffe", Ph.D. Thesis, University of Karlsruhe, 1992.
10. E. Wernick, *Bautechnik* **8**, 263-267 (1977).
11. Wernick, *Bautechnik* **8**, 263-267 (1977).